

Exploring Metallic-Insulating Transition and Thermodynamic Applications of Fibonacci Quasicrystals

He-Guang Xu¹ and Shujie Cheng^{2,3,*}

¹*School of Physics, Dalian University of Technology, 116024 Dalian, China*

²*Xingzhi College, Zhejiang Normal University, Lanxi 321100, China*

³*Department of Physics, Zhejiang Normal University, Jinhua 321004, China*

(Dated: October 24, 2024)

Extended and critical states are two common phenomena in Fibonacci quasicrystals. In this paper, we first reveal the difference between the extended phase and the critical phase in the extended-critical Fibonacci quasicrystal from the perspectives of quantum transport and Wigner distribution. The transport conductance indicates that the extended-critical transition resembles a metallic-insulating transition. Moreover, the Wigner distributions show that the Wigner distribution of the extended wave function is localized in the momentum direction of the phase space, while that of the critical wave function is sub-extended in the momentum direction of the phase space. Based on the results of entanglement entropy, the extended-critical transition is a thermodynamic phase transition because it is accompanied by decreasing entropy. We engineer a quantum heat cycle engine with the extended-critical quasicrystal as the working medium, and find that there are rich working modes in the engine, such as quantum accelerator, quantum heater and quantum heat engine. Importantly, the extended quasicrystals are more conducive to the realization of quantum heat engines, while the critical quasicrystals are more conducive to the realization of quantum heaters. Our work is an important step toward exploring the rich thermodynamic applications of Fibonacci quasicrystals.

I. INTRODUCTION

Anderson localization is a widely studied quantum phenomenon that exists in quantum systems with disorder or quasidisorder and explains how matter waves appear to lack ergodicity in such disordered [1] or quasidisordered environments [2]. Its influence extends to a wide range of physical disciplines, including condensed matter physics [3, 4], which helps elucidate the properties of electrons in disordered materials. In ultra-cold atomic systems, the study of Anderson localization has also been crucial in helping to understand the effects of complex disordered environments on particle behavior and driving the development of optical lattice experimental design and measurement techniques [5–15]. In addition, the study of Anderson localization in photonic crystals will help understand the transmission behavior of light and promote the development of functional optical devices [16–22].

Under different physical mechanisms, Anderson localization presents different forms. For example, in the Fibonacci quasicrystal, when the strength of the quasidisordered potential exceeds to the critical value, all quantum states are localized [2, 6]. However, in the three-dimensional Anderson model [3] or in systems with short-(long-) range hoppings [23–30], and generalized quasidisordered potentials [31–39], Anderson localization occurs only at certain energy levels, separated from the delocalized energy levels by the mobility edge. This makes the overall nature of the system appear to be in an intermediate phase that is neither fully extended nor fully localized. Based on the researches of mobility edge, the inter-

mediate phase with extended-localized mobility edge has been found, which are used for the realizations of energy current rectification [40] and superradiance light sources [41]. In addition, it has been found that the electrical transport properties of the system can be significantly affected by properly designing and controlling the interaction between the system and the environment. This makes it possible to induce or annihilate the mobility edge through the interaction of the system with the environment, thereby altering the metallic or insulating properties of the system. For example, Liu et al. recently investigated the effect of bond dissipation on the Fibonacci quasicrystal with mobility edges and found that this dissipation mechanism can destroy mobility edges, causing the system to be fully extended or fully localized in non-equilibrium steady-state [42]. Here the extended-localized transition leads to the metallic-insulating transition of the system. Very recently, Longhi studied the influence of dephasing effects on Fibonacci quasicrystals with mobility edges and found that mobility edges do not disappear under dephasing effects. Meanwhile, the influence of dephasing on the off-diagonal Fibonacci quasicrystal with extended-critical phase transition was also studied, and the unexpected mobility edge induced by the dephasing effect was found [43]. Although the wave function of the critical phase is sub-extended, it remains to be emphasized whether the critical quasicrystals behave more like metals or insulators in the transport measurements. Meanwhile, we note that the attentions are more payed to the localization physics of Fibonacci quasicrystals at zero temperature. In fact, it has been shown that Fibonacci quasicrystals with mobility edges interacting

with external heat baths can be used to engineer quantum heat engines [44]. However, for the Fibonacci quasicrystal without mobility edge, whether the interaction with the external heat source will trigger the quantum heat engine or richer applications remain to be explored.

The paper is organized as follows. In Sec. III, we introduce the Hamiltonian of the Fibonacci quasicrystal and study its electrical transport properties. In Sec. IV, we reveal the localization properties from the aspects of Wigner distribution and entanglement entropy. In Sec. V, we explore the thermodynamic application of Fibonacci Quasicrystal. A summary is made in Sec. ??.

II. MODEL AND ELECTRICAL TRANSPORT PROPERTIES

We consider the off-diagonal Fibonacci quasicrystal described by the following Hamiltonian

$$\hat{H} = - \sum_n \left(t_n \hat{c}_{n+1}^\dagger \hat{c}_n + \text{H.c.} \right), \quad (1)$$

in which $t_n = t + t_1 \cos(2\pi\alpha n + \varphi)$ (where t is the unit the energy) denotes the incommensurate hopping amplitude (The commensuration is reflected in that the frequency α is the ratio of two adjacent infinite Fibonacci numbers.) between nearest neighbor sites n and $(n + 1)$ and $\hat{c}_n, \hat{c}_n^\dagger$ are the annihilation and creation operators of the hard-core bosons at site n . The model presents extended-critical transition with the critical value $t_c = t$, and the phase diagram is shown in Fig. 1. Refs. [15, 43, 45–47] give the early proof of extended-critical transition in off-diagonal quasicrystals from perspectives of (inverse) participation ratio, fractal dimension, and the spreading dynamics. When $t_1 < t_c$, the system is in the extended phase, and when $t_1 > t_c$, the system is in the critical phase. In fact, the extended-critical transition can be understood by means of quantum transport measurement as well, which gives the transport conductance of the off-diagonal quasicrystal, the most direct characterization of the electrical transport properties of the systems. Although the wave function in the critical phase is sub-extended, it remains to be explored whether the critical quasicrystals behave more like metals or insulators in terms of their transport properties.

Solving the conductance by quantum scattering is a feasible method in quantum transport theory [48, 49], which is used to study the transport properties of electrons in quantum systems. In the following, we will briefly describe how to solve the transport conductance of this non-diagonal quasicrystal by the quantum scattering method. By engineering a quantum transport device composed of a source, non-diagonal quasicrystals and a drain, and making incoming electrons with energy E experience the process of transmission, reflection from

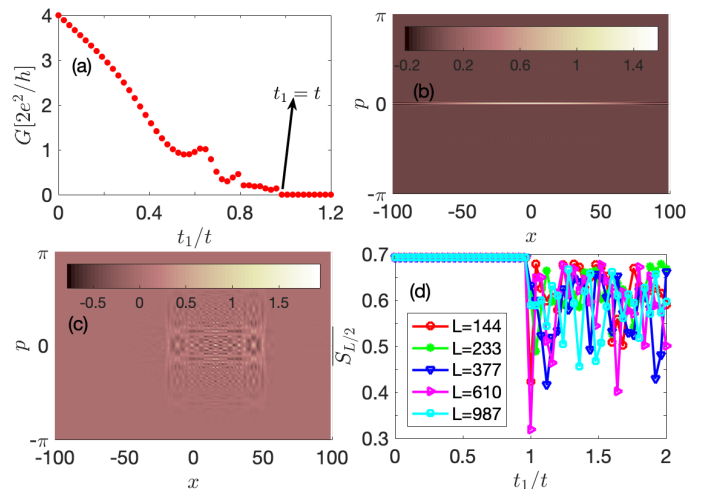


Figure 1. (Color online) (a) Transport conductance as a functions of t_1 . The system size is $L = 987$ and the incoming energy is $E = 0.01t$. (b) The Wigner distribution of the ground state under $L = 200$ and $t_1 = 0.2t$. (c) The Wigner distribution of the ground state under $L = 200$ and $t_1 = 1.2t$. (d) The mean single-particle entanglement entropy $\bar{S}_{1/2}$ as a function of t_1 .

source to drain, and scattering with a off-diagonal quasicrystals, we can obtain the quantum scattering matrix of the transport process, which is defined as

$$S = \begin{pmatrix} R & T' \\ T & R' \end{pmatrix} \quad (2)$$

in which R and R' denote the reflection matrices while T and T' denote the transmission.

The conductance (G) can be calculated by the transmission matrix T . In quantum transport theory, the conductance is related to the trace of T . Under an incoming energy E , G is defined as

$$G = \frac{2e^2}{h} \text{Tr} [TT^\dagger], \quad (3)$$

where e^2/h is the unit of G and the factor 2 stands for the spin degeneracy. Considering the incoming energy $E = 0.01t$, the conductance G as a function of the hopping parameter t_1 is plotted in Fig. 1(a). As seen, when the off-diagonal quasicrystal undergoes the transition from the extended phase to the critical phase, there is an accompanying vanishing transport conductance.. It means that the extended-critical transition in the off-diagonal quasicrystal is more like a metallic-insulating transition. In this regard, in addition to the extended-localized quasicrystals, the extended-critical quasicrystal can be used as a quantum current limiter as well.

III. WINGER DISTRIBUTION AND ENTANGLEMENT ENTROPY

In addition to the quantum transport, the difference between the extended and critical phase can be readily seen from the Wigner distribution [50–53]. The Wigner distribution function provides a way to describe quantum states in phase space. It maps the wave function of the quantum state to a real function of the phase space, so that the distribution of the quantum state can be intuitively understood in the phase space. For a given wave function $\psi(x)$ (where x is the position), the corresponding Wigner distribution function $W(x, p)$ (p is the momentum) is defined as

$$W(x, p) = \frac{1}{2\pi\hbar} \int_{-\infty}^{+\infty} \psi(x + \frac{y}{2})\psi(x - \frac{y}{2})e^{-ipy/\hbar} dy, \quad (4)$$

Considering the system size $L = 200$, the ground-states (chosen as examples) $W(x, p)$ under $t_1 = 0.2t$ and $t_1 = 1.2t$ are plotted in Figs. 1(b) and 1(c), respectively. The extended ground state corresponds to the extended distribution in the x direction and the localized distribution in the p direction in the phase space. The critical ground state corresponds to the sub-extended distribution in the x and p directions in the phase space. In addition, it can be seen that in some regions in the phase space, $W(x, p)$ are positive, while in others, the distributions are negative. Therefore, the results not only explain the extension-critical difference, but also reveal the property of Wigner distribution function as a quasi-probability distribution function.

We reveal that the extended-critical transition is actually a thermodynamic phase transition. We here detect the thermodynamic property by the thermodynamic quantity, i.e., single particle entanglement entropy $S_{L/2}$, which is defined as

$$S_{L/2} = - \sum_j [\epsilon_j \ln \epsilon_j + (1 - \epsilon_j) \ln(1 - \epsilon_j)], \quad (5)$$

where the ϵ_j is the eigenvalues of the half-chain single-particle correlation matrix C , given by

$$C_{mn} = \langle \psi | \hat{c}_m^\dagger \hat{c}_n | \psi \rangle, \quad (6)$$

with $|\psi\rangle$ the wave function. Taking different system size, the mean single-particle entanglement entropy $\bar{S}_{L/2}$ as functions of t_1 are plotted in Fig. 1(d). We can see that, when the hopping parameter t_1 exceeds the extended-critical transition point, there are decreasing single-particle entanglement entropy. In previous study, the realization of quantum heat engine is often accompanied by the high entropy state of the working medium [53]. Thus, we speculate that here the extended quasicrystal is beneficial to the realization of the quantum heat engine. Notice that in the critical phase, $\bar{S}_{L/2}$ is only

slightly lower than that in the extended phase, but it does not approach zero. Therefore, the underlying applications brought by the critical quasicrystal is an open question to be solved. Even in the extended phase, whether there are applications other than quantum heat engine is also worth exploring.

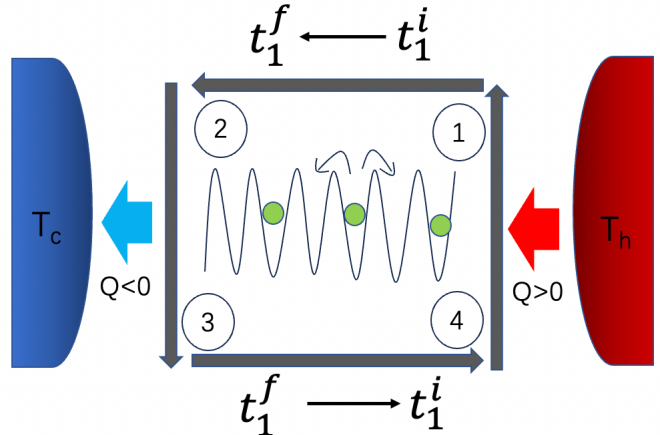


Figure 2. (Color online) Sketch of the four-strokes quantum heat cycle process. T_h and T_c denote the high temperature and low temperature heat sources, respectively. The working medium is the extended-critical quasicrystal. t_1^f and t_1^i are the hopping parameters of corresponding Hamiltonians.

IV. QUANTUM HEAT CYCLE

We engineer a quantum heat cycle process using the extended-critical quasicrystal as the working medium, and the schematic diagram is displayed in Fig. 2. This heat cycle process can be viewed as the quantum analog [53–65] of the classical Otto cycle. The first ($\textcircled{4} \rightarrow \textcircled{1}$) and third ($\textcircled{2} \rightarrow \textcircled{3}$) strokes take place in heat contact with high (T_h) and low (T_c) temperature heat sources and run without external driving. The second ($\textcircled{1} \rightarrow \textcircled{2}$) and fourth ($\textcircled{3} \rightarrow \textcircled{4}$) strokes are adiabatic from a thermodynamic perspective (meaning they are isolated from heat), but they may not be adiabatic in a quantum-mechanical sense, as quantum transitions can take place during the evolution [64].

In the first stroke, the working medium with the Hamiltonian $H(t_1^i)$ will finally relax into the Gibbs state of thermal equilibrium, whose density matrix ρ_1 is given by $\rho_1 = \frac{e^{-\beta_h H(t_1^i)}}{Z_1}$ with $\beta_h = \frac{1}{k_b T_h}$ and partition function $Z_1 = \text{Tr}(e^{-\beta_h H(t_1^i)})$. Thus, in the thermal equilibrium, the energy of the system is $E_1 = \text{Tr}[\rho_1 H(t_1^i)]$. During the second stroke, the Hamiltonian parameter is changed from t_1^i to t_1^f and only work is performed without any heat being exchanged. The Gibbs state of this stroke ρ_2 remain unchanged, i.e., $\rho_2 = \rho_1$, but the energy E_2

becomes $E_2 = \text{Tr} [\rho_2 H(t_1^f)]$. In the third stroke, the medium with $t_1 = t_1^f$ is in contact with the source $\beta_c = \frac{1}{k_b T_c}$. Hence, the Gibbs state ρ_3 gives $\rho_3 = e^{-\beta_c H(t_1^f)} / Z_2$ with partition function $Z_2 = \text{Tr} [e^{-\beta_c H(t_1^f)}]$. Then, the energy of the medium E_3 is $E_3 = \text{Tr} [\rho_3 H(t_1^f)]$. The fourth stroke can be viewed as the quantum annealing process. In this process, the hopping parameter in the medium is changed from t_1^f back to t_1^i . However, the Gibbs state ρ_4 remains $\rho_4 = \rho_3$. Therefore, the energy of medium becomes $E_4 = \text{Tr} [\rho_4 H(t_1^i)]$. After the working medium has experienced this complete cycle process, we can obtain the absorbed heat Q_h from the T_h source, and the released heat Q_c to the T_c source, as well as the net work W of the working medium $W = Q_h + Q_c$. Importantly, this heat cycle process obeys the Clausius inequality, which is one of the cornerstones of thermodynamics. According to different values of Q_1 , Q_2 , and W , the engine with extended-critical quasicrystal as the working medium will present different modes [63, 64]: (1) *Heat engine*: $Q_h > 0$, $Q_c < 0$, and $W > 0$; (2) *Refrigerator*: $Q_h < 0$, $Q_c > 0$, and $W < 0$; (3) *Heater*: $Q_h < 0$, $Q_c < 0$, and $W < 0$; (4) *Accelerator*: $Q_h > 0$, $Q_c < 0$, and $W < 0$.

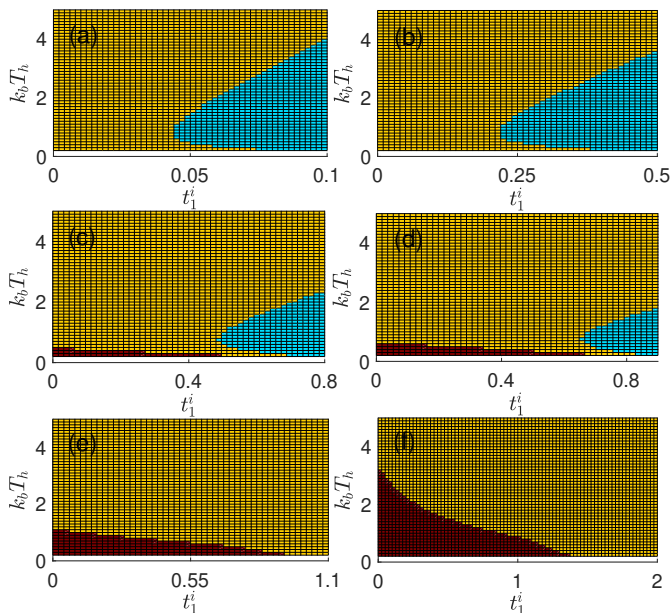


Figure 3. (Color online) Modes of the four-stroke engine in the $k_b T_h - t_1^i$ parameter plane. (a) $t_1^f = 0.1t$. (b) $t_1^f = 0.5t$. (c) $t_1^f = 0.8t$. (d) $t_1^f = 0.9t$. (e) $t_1^f = 1.1t$. (f) $t_1^f = 2t$. The blue regions denote the *Heat engine*. The yellow regions denote the *Accelerator* and the brown regions denote the *Heater*. Other parameters are $L = 233$ and $k_b T_c = 0.1t$.

Taking the system size $L = 233$ and $k_b T_c = 0.1t$, after analyzing the values of Q_1 , Q_2 , and W , the corresponding modes of the four-stroke engine with t_1^f equal-

ing to $0.1t$, $0.5t$, $0.8t$, $0.9t$, $1.1t$, and $2t$ are plotted in Figs. 3(a)-3(f), respectively. We can see that this engine with extended-critical quasicrystal as the working medium has rich working modes. The blue regions denote the *Heat engine*. The yellow regions denote the *Accelerator* and the brown regions denote the *Heater*. We note that when t_1^f and t_1^i are less than the critical value t_c , there is the mode of *Heat engine*, as the blue regions show. It means that the extended quasicrystal are more conducive to the design of quantum heat engine. When t_1^f gradually gets larger, and exceeds the critical values, we can see that the regions characterizing the mode of the *Heater* get larger as well. It means that the critical quasicrystal are more conducive to the realization of the quantum heater. Besides, it is evident that there are extensive parameter regions that characterize the mode of the *Accelerator*, regardless of whether the quasicrystal is in the extended phase or the critical phase. It implies that the extended and critical quasicrystals are both conducive to the realization of the quantum accelerator.

In addition, the results presented in Fig. 3 provide strategies for regulating the working mode of the four-stroke engine as well. The transition between different working modes can be achieved by adjusting t_1^f , t_1^i , and $k_b T_h$. For instance, when t_1^f is far less than t_c (see Figs. 3(a) and 3(b)), one can adjust t_1^i or $k_b T_h$ to make the working mode of the engine change from the *Accelerator* to the *Heat engine*, or from the *Heat engine* to the *Accelerator*, respectively. When t_1^f is close to but still less than t_c , there are three working modes when $k_b T_h$ is small. Therefore, the working mode of the engine will change from the *Heater* to the *Accelerator* and then to the *Heat engine*. When t_1^f is larger than t_c , the engine can be switched between heater and accelerator by adjusting t_1^i or $k_b T_h$.

V. SUMMARY

In summary, we have revealed that the extended-critical Fibonacci quasicrystal presents metallic-insulating transition from the perspective of quantum transport. Besides, there is a quantum-classical correspondence between the wave function and the Wigner distribution in phase space. Specifically, the extended wave function corresponds to the localized Wigner distribution in the momentum direction in the phase space, while the critical wave function corresponds to the sub-extended distribution in the momentum direction. Importantly, the single-particle entanglement entropy shows that the extended-critical transition is actually a thermodynamic transition, due to the decrease of the entanglement entropy when the Fibonacci quasicrystal goes from the extended phase to the critical phase. The thermodynamic transition leads to rich applications of the quantum Otto heat cycle engine with

extended-critical Fibonacci quasicrystal being the working medium, including quantum heat engine, quantum accelerator, and the quantum heater. Interestingly, the extended Fibonacci quasicrystal are more conductive to be employed to engineer the quantum heat engine, while the critical Fibonacci quasicrystal are more conductive to be employed to engineer the quantum heater. Both the extended and critical phase are conductive to the realization of quantum accelerator. By adjusting the quasicrystal parameters and the temperature of the heat source, we can realize the transition between different working modes.

This work is supported by the start-up fund from Xingzhi college, Zhejiang Normal University.

* chengsj@zjnu.edu.cn

- [1] P. W. Anderson, "Absence of diffusion in certain random lattices," *Phys. Rev.* **109**, 1492–1505 (1958).
- [2] S. Aubry and G. André, "Analyticity breaking and anderson localization in incommensurate lattices," *Ann. Israel Phys. Soc.* **3**, 133 (1980).
- [3] N. Mott, "The mobility edge since 1967," *J. Phys. C: Solid State Phys.* **20**, 3075–3102 (1987).
- [4] F. Evers and Alexander D. Mirlin, "Anderson transitions," *Rev. Mod. Phys.* **80**, 1355–1417 (2008).
- [5] L. Sanchez-Palencia, D. Clément, P. Lugan, P. Bouyer, G. V. Shlyapnikov, and A. Aspect, "Anderson localization of expanding bose-einstein condensates in random potentials," *Phys. Rev. Lett.* **98**, 210401 (2007).
- [6] G. Roati, C. D'Errico, L. Fallani, M. Fattori, C. Fort, M. Zaccanti, G. Modugno, M. Modugno, and M. Inguscio, "Anderson localization of a non-interacting bose-einstein condensate," *Nature* **453**, 895–898 (2008).
- [7] J. Billy, V. Josse, Z. Zuo, A. Bernard, B. Hambrecht, P. Lugan, D. Clément, L. Sanchez-Palencia, P. Bouyer, and A. Aspect, "Direct observation of anderson localization of matter waves in a controlled disorder," *Nature* **453**, 891–894 (2008).
- [8] S. S. Kondov, W. R. McGehee, J. J. Zirbel, and B. DeMarco, "Three-dimensional anderson localization of ultra-cold matter," *Science* **334**, 66–68 (2011).
- [9] F. Jendrzejewski, A. Bernard, K. Müller, P. Cheinet, V. Josse, M. Piraud, L. Pezzé, L. Sanchez-Palencia, A. Aspect, and P. Bouyer, "Three-dimensional localization of ultracold atoms in an optical disordered potential," *Nat. Phys.* **8**, 398–404 (2012).
- [10] G. Semeghini, M. Landini, P. Castilho, S. Roy, G. Spagnolli, A. Trenkwalder, M. Fattori, M. Inguscio, and G. Modugno, "Measurement of the mobility edge for 3d anderson localization," *Nat. Phys.* **11**, 554–559 (2015).
- [11] D. Delande and G. Orso, "Mobility edge for cold atoms in laser speckle potentials," *Phys. Rev. Lett.* **113**, 060601 (2014).
- [12] L. Sanchez-Palencia, "Ultracold gases: At the edge of mobility," *Nat. Phys.* **11**, 525–526 (2015).
- [13] H. P. Lüschen, S. Scherg, T. Kohert, M. Schreiber, P. Bordia, X. Li, S. Das Sarma, and I. Bloch, "Single-particle mobility edge in a one-dimensional quasiperiodic optical lattice," *Phys. Rev. Lett.* **120**, 160404 (2018).
- [14] F. Alex An, K. Padavic, E. J. Meier, S. Hegde, S. Ganeshan, J. H. Pixley, S. Vishveshwara, and B. Gadway, "Observation of a topological phase with critical localization in a quasi-periodic lattice," *Phys. Rev. Lett.* **126**, 040603 (2021).
- [15] T. Xiao, D. Xie, Z. Dong, T. Chen, W. Yi, and B. Yan, "Observation of topological phase with critical localization in a quasi-periodic lattice," *Sci. Bull.* **66**, 2175–2180 (2021).
- [16] D. S. Wiersma, P. Bartolini, A. Lagendijk, and R. Righini, "Localization of light in a disordered medium," *Nature* **390**, 671–673 (1997).
- [17] T. Schwartz, G. Bartal, S. Fishman, and M. Segev, "Transport and anderson localization in disordered two-dimensional photonic lattices," *Nature* **446**, 52–55 (2007).
- [18] Y. Lahini, A. Avidan, F. Pozzi, M. Sorel, R. Morandotti, D. N. Christodoulides, and Y. Silberberg, "Anderson localization and nonlinearity in one-dimensional disordered photonic lattices," *Phys. Rev. Lett.* **100**, 013906 (2008).
- [19] D. S. Wiersma, "Disordered photonics," *Nat. Photon.* **7**, 188–196 (2013).
- [20] M. Segev, Y. Silberberg, and D. N. Christodoulides, "Anderson localization of light," *Nat. Photon.* **7**, 197–204 (2013).
- [21] H. E. Kondakci, A. F. Abouraddy, and B. E. A. Saleh, "A photonic thermalization gap in disordered lattices," *Nat. Phys.* **11**, 930–936 (2015).
- [22] S. Yu, C.-W. Qiu, Y. Chong, S. Torquato, and N. Park, "Engineered disorder in photonics," *Nat. Rev. Mat.* **6**, 226–243 (2021).
- [23] J. Biddle and S. Das Sarma, "Predicted mobility edges in one-dimensional incommensurate optical lattices: An exactly solvable model of anderson localization," *Phys. Rev. Lett.* **104**, 070601 (2010).
- [24] X. Deng, S. Ray, S. Sinha, G. V. Shlyapnikov, and L. Santos, "One-dimensional quasicrystals with power-law hopping," *Phys. Rev. Lett.* **123**, 025301 (2019).
- [25] N. Roy and A. Sharma, "Fraction of delocalized eigenstates in the long-range aubry-andré-harper model," *Phys. Rev. B* **103**, 075124 (2021).
- [26] J. Biddle, D. J. Priour, B. Wang, and S. Das Sarma, "Localization in one-dimensional lattices with non-nearest-neighbor hopping: Generalized anderson and aubry-andré models," *Phys. Rev. B* **83**, 075105 (2011).
- [27] Y. Liu, Y. Wang, Z. Zhang, and S. Chen, "Exact non-hermitian mobility edges in one-dimensional quasicrystal lattice with exponentially decaying hopping and its dual lattice," *Phys. Rev. B* **103**, 134208 (2021).
- [28] M. Saha, S. K. Maiti, and A. Purkayastha, "Anomalous transport through algebraically localized states in one dimension," *Phys. Rev. B* **100**, 174201 (2019).
- [29] Z. Xu, X. Xia, and S. Shu, "Non-hermitian aubry-andré model with power-law hopping," *Phys. Rev. B* **104**, 224204 (2021).
- [30] L.-Z. Tang, G.-Q. Zhang, L.-F. Zhang, and D.-W. Zhang, "Localization and topological transitions in non-hermitian quasiperiodic lattices," *Phys. Rev. A* **103**, 033325 (2021).
- [31] S. Das Sarma, S. He, and X. C. Xie, "Mobility edge in a model one-dimensional potential," *Phys. Rev. Lett.* **61**, 2144–2147 (1988).
- [32] S. Ganeshan, J. H. Pixley, and S. Das Sarma, "Near-

- est neighbor tight binding models with an exact mobility edge in one dimension,” *Phys. Rev. Lett.* **114**, 146601 (2015).
- [33] H. Yao, H. Khoudli, L. Bresque, and L. Sanchez-Palencia, “Critical behavior and fractality in shallow one-dimensional quasiperiodic potentials,” *Phys. Rev. Lett.* **123**, 070405 (2019).
- [34] T. Liu and H. Guo, “Mobility edges in off-diagonal disordered tight-binding models,” *Phys. Rev. B* **98**, 104201 (2018).
- [35] Y. Wang, X. Xia, L. Zhang, H. Yao, S. Chen, J. You, Q. Zhou, and X.-J. Liu, “One dimensional quasiperiodic mosaic lattice with exact mobility edges,” *Phys. Rev. Lett.* **125**, 196604 (2020).
- [36] T. Liu, X. Xia, S. Longhi, and L. Sanchez-Palencia, “Anomalous mobility edges in one-dimensional quasiperiodic models,” *SciPost Phys.* **12**, 027 (2022).
- [37] X.-C. Zhou, Y. Wang, T.-F. J. Poon, Q. Zhou, and X.-J. Liu, “Exact new mobility edges between critical and localized states,” *Phys. Rev. Lett.* **131**, 176401 (2023).
- [38] T. Liu, H. Guo, Y. Pu, and S. Longhi, “Generalized Aubry-André self-duality and mobility edges in non-hermitian quasiperiodic lattices,” *Phys. Rev. B* **102**, 024205 (2020).
- [39] Y. Liu, Y. Wang, X.-J. Liu, Q. Zhou, and S. Chen, “Exact mobility edges, pt -symmetry breaking and skin effect in one-dimensional non-hermitian quasicrystals,” *Phys. Rev. B* **103**, 014203 (2021).
- [40] V. Balachandran, S. R. Clark, J. Goold, and D. Poletti, “Energy current rectification and mobility edges,” *Phys. Rev. Lett.* **123**, 020603 (2019).
- [41] H. Yin, J. Hu, A.-C. Ji, G. Juzeliunas, X.-J. Liu, and Q. Sun, “Localization driven superradiant instability,” *Phys. Rev. Lett.* **124**, 113601 (2020).
- [42] Y. Liu, Z. Wang, C. Yang, J. Jie, and Y. Wang, “Dissipation-induced extended-localized transition,” *Phys. Rev. Lett.* **132**, 216301 (2024).
- [43] S. Longhi, “Dephasing-induced mobility edges in quasicrystals,” *Phys. Rev. Lett.* **132**, 236301 (2024).
- [44] C. Chiaracane, M. T. Mitchison, A. Purkayastha, G. Haack, and J. Goold, “Quasiperiodic quantum heat engines with a mobility edge,” *Phys. Rev. Res.* **2**, 013093 (2020).
- [45] I. Chang, K. Ikezawa, and M. Kohmoto, “Multifractal properties of the wave functions of the square-lattice tight-binding model with next-nearest-neighbor hopping in a magnetic field,” *Phys. Rev. B* **55**, 12971 (1997).
- [46] Y. E. Kraus, Y. Lahini, Z. Ringel, M. Verbin, and O. Zeitler, “Topological states and adiabatic pumping in quasicrystals,” *Phys. Rev. Lett.* **109**, 106402 (2012).
- [47] T. Liu, P. Wang, and X. Gao, “Phase diagram of the off-diagonal Aubry-André model,” *arXiv* (2016), 1609.06939.
- [48] S. Datta, *Electronic Transport in Mesoscopic Systems* (Cambridge University Press, England, 1995).
- [49] P. W. Brouwer, P. G. Silvestrov, and C. W. J. Beenakker, “Theory of direct localization in one dimension,” *Phys. Rev. B* **56**, R4333(R) (1997).
- [50] E. Wigner, “On the quantum correction for thermodynamic equilibrium,” *Phys. Rev.* **40**, 749 (1932).
- [51] H. Y. Fan, “Thermal Wigner operator in coherent thermal state representation and its application,” *Commun. Theor. Phys.* **37**, 289 (2002).
- [52] M. Reboiro, O. Civitarese, and D. Tielas, “Use of discrete Wigner function in the study of decoherence of a system of superconducting flux-qubits,” *Phys. Scr.* **90**, 074028 (2015).
- [53] H. T. Quan, Y.-X. Liu, C. P. Sun, and F. Nori, “Quantum thermodynamics cycles and quantum heat engines,” *Phys. Rev. E* **76**, 031105 (2007).
- [54] A. O. Niskanen, Y. Nakamura, and J. P. Pekola, “Information entropic superconducting microcooler,” *Phys. Rev. B* **76**, 174523 (2007).
- [55] O. Abah, J. Roßnagel, G. Jacob, S. Deffner, F. Schmidt-Kaler, K. Singer, and E. Lutz, “Single-atom heat engine,” *Phys. Rev. Lett.* **109**, 203006 (2012).
- [56] J. Deng, Q.-H. Wang, Z. Liu, P. Hänggi, and J. Gong, “Quantum Otto engines with finite-time discontinuities,” *Phys. Rev. E* **88**, 062122 (2013).
- [57] A. del Campo, J. Goold, and M. Paternostro, “More bang for your buck: Super-adiabatic quantum engines,” *Sci. Rep.* **4**, 6208 (2014).
- [58] J. Roßnagel, S. T. Dawkins, K. N. Tolazzi, Q. Abah, E. Lutz, F. Schmidt-Kaler, and K. Singer, “A single-atom heat engine,” *Science* **352**, 325 (2016).
- [59] Y. Zheng, P. Hänggi, and D. Poletti, “Occurrence of discontinuities in the performance of finite-time quantum Otto cycles,” *Phys. Rev. E* **94**, 012137 (2016).
- [60] R. Kosloff and Y. Rezek, “The quantum harmonic Otto cycle,” *Entropy* **19**, 136 (2017).
- [61] S. Deffner and S. Campbell, *Quantum Thermodynamics* (Morgan Claypool Publishers, 2019).
- [62] M. Campisi and R. Fazio, “The power of a critical heat engine,” *Nat. Commun.* **7**, 11895 (2016).
- [63] L. Buffoni, A. Solfanelli, P. Verrucchi, A. Cuccoli, and M. Campisi, “Quantum measurement cooling,” *Phys. Rev. Lett.* **122**, 070603 (2019).
- [64] A. Solfanelli, M. Falsetti, and M. Campisi, “Nonadiabatic single-qubit quantum Otto engine,” *Phys. Rev. B* **101**, 054513 (2020).
- [65] J. W. Zhang, J. Q. Zhang, G.-Y. Ding, J.-C. Li, J.-T. Bu, B. Wang, L.-L. Yan, S.-L. Su, L. Chen, F. Nori, S. K. Özdemir, F. Zhou, H. Jing, and M. Feng, “Dynamical control of quantum heat engines using exceptional points,” *Nat. Commun.* **13**, 6225 (2022).